

# Optimized arylomycins are a new class of Gram-negative antibiotics

Peter A. Smith<sup>1,15\*</sup>, Michael F. T. Koehler<sup>2,15</sup>, Hany S. Grgis<sup>1</sup>, Donghong Yan<sup>3</sup>, Yongsheng Chen<sup>4</sup>, Yuan Chen<sup>5</sup>, James J. Crawford<sup>2</sup>, Matthew R. Durk<sup>5</sup>, Robert I. Higuchi<sup>6,11</sup>, Jing Kang<sup>3</sup>, Jeremy Murray<sup>7</sup>, Prasuna Paraselli<sup>6,12</sup>, Summer Park<sup>3</sup>, Wilson Phung<sup>8</sup>, John G. Quinn<sup>9</sup>, Tucker C. Roberts<sup>6,13</sup>, Lionel Rouge<sup>7</sup>, Jacob B. Schwarz<sup>2,14</sup>, Elizabeth Skippington<sup>10</sup>, John Wai<sup>4</sup>, Min Xu<sup>3</sup>, Zhiyong Yu<sup>4</sup>, Hua Zhang<sup>3</sup>, Man-Wah Tan<sup>1</sup> & Christopher E. Heise<sup>1,9\*</sup>

Multidrug-resistant bacteria are spreading at alarming rates, and despite extensive efforts no new class of antibiotic with activity against Gram-negative bacteria has been approved in over fifty years. Natural products and their derivatives have a key role in combating Gram-negative pathogens. Here we report chemical optimization of the arylomycins—a class of natural products with weak activity and limited spectrum—to obtain G0775, a molecule with potent, broad-spectrum activity against Gram-negative bacteria. G0775 inhibits the essential bacterial type I signal peptidase, a new antibiotic target, through an unprecedented molecular mechanism. It circumvents existing antibiotic resistance mechanisms and retains activity against contemporary multidrug-resistant Gram-negative clinical isolates in vitro and in several in vivo infection models. These findings demonstrate that optimized arylomycin analogues such as G0775 could translate into new therapies to address the growing threat of multidrug-resistant Gram-negative infections.

The discovery and development of several classes of safe and efficacious antibiotics has markedly reduced mortality from bacterial infections. However, the overuse and misuse of these same antibiotics—both in medicine and in agriculture—has driven the rapid evolution and dissemination of antibiotic resistance<sup>1</sup>. The ‘ESKAPE’ pathogens (*Enterococcus faecium*, *Staphylococcus aureus*, *Klebsiella pneumoniae*, *Acinetobacter baumannii*, *Pseudomonas aeruginosa* and *Enterobacter* species)<sup>2</sup> present the most acute threat of developing untreatable multidrug-resistant (MDR) infections, with the Gram-negative members of this group (*Escherichia coli*, *K. pneumoniae*, *P. aeruginosa* and *A. baumannii*) posing a particular threat owing to their dual-membrane envelope that prevents many antibiotics from accessing their targets. Despite considerable effort, no new class of antibiotic has been approved for Gram-negative pathogens in over fifty years.

The arylomycins are a class of macrocyclic lipopeptides<sup>3,4</sup> that inhibit the bacterial type I signal peptidase (SPase), an essential membrane-bound protease that uses an atypical serine–lysine dyad to cleave signal sequences from pre-proteins following their translocation across the cytoplasmic membrane<sup>5</sup>. SPase has been pursued as an antibiotic target for nearly twenty years<sup>6–9</sup>, with a focus on developing agents with activity against Gram-positive bacteria, in which the active site of the enzyme is exposed on the surface of the cell. In Gram-negative bacteria the active site of SPase is located in the periplasmic space between the cytoplasmic membrane and the outer membrane, and was thought to be inaccessible to the arylomycins because their high molecular weight and lipophilicity would preclude penetration of the outer membrane<sup>10–12</sup>. Consistent with this hypothesis, no member of the arylomycin class has shown activity against the Gram-negative ESKAPE pathogens. It has been demonstrated that arylomycins have some intrinsic ability to penetrate the outer membrane, and that their lack of activity against

Gram-negative pathogens is attributable in part to a naturally occurring mutation in the Gram-negative SPase LepB that reduces the binding affinity of arylomycin<sup>13,14</sup>. Encouraged by these results, we initiated a systematic optimization effort to identify arylomycin analogues with increased target affinity and improved penetration of the outer membrane. Here we describe the discovery of G0775, a synthetic arylomycin derivative with potent in vitro antibacterial activity against the Gram-negative ESKAPE pathogens. Notably, the physicochemical properties of G0775 remain outside the range that is currently considered conducive to yielding potent Gram-negative activity, which suggests that it uses an atypical mechanism to penetrate the outer membrane. Crucially, highly MDR pathogens that are resistant to nearly all available antibiotic therapies are susceptible to G0775, and de novo resistance to G0775 occurs at a low frequency. The potent in vitro activity of G0775 translates into robust in vivo efficacy in several infection models, demonstrating the potential of these optimized natural products to address the growing clinical threat of antibiotic resistant Gram-negative bacteria.

## Optimized arylomycins have Gram-negative activity

Arylomycins consist of a macrocyclic tripeptide core with an N-terminal lipopeptide tail (purple), a C-terminal carboxylic acid (green) and two phenols on the aromatic rings of the macrocycle (red), as shown in Fig. 1. With the aim of modifying this natural scaffold into a broadly active Gram-negative antibiotic, we explored modifications at all three regions. Because crystal structures of the Gram-negative SPase LepB in complex with arylomycin indicate that the macrocyclic core preorganizes the peptide backbone and occupies a conserved region of the substrate-binding pocket<sup>15,16</sup>, we chose to leave this region unchanged. Naturally occurring variants of the arylomycin N-terminal lipopeptide tail are known to modulate the spectrum of activity against

<sup>1</sup>Department of Infectious Diseases, Genentech, South San Francisco, CA, USA. <sup>2</sup>Department of Discovery Chemistry, Genentech, South San Francisco, CA, USA. <sup>3</sup>Department of Translational Immunology, Genentech, South San Francisco, CA, USA. <sup>4</sup>Department of Chemistry, Wuxi AppTec, Shanghai, China. <sup>5</sup>Department of Drug Metabolism and Pharmacokinetics, Genentech, South San Francisco, CA, USA. <sup>6</sup>RQx Pharmaceuticals, La Jolla, CA, USA. <sup>7</sup>Department of Structural Biology, Genentech, South San Francisco, CA, USA. <sup>8</sup>Department of Microchem Proteomics, Genentech, South San Francisco, CA, USA. <sup>9</sup>Department of Biochemical and Cellular Pharmacology, Genentech, South San Francisco, CA, USA. <sup>10</sup>Department of Bioinformatics and Computational Biology, Genentech, South San Francisco, CA, USA. <sup>11</sup>Present address: Retrovirox, San Diego, CA, USA. <sup>12</sup>Present address: Vertex, San Diego, CA, USA. <sup>13</sup>Present address: Aduro Biotech, Berkeley, CA, USA. <sup>14</sup>Present address: FLX Bio, South San Francisco, CA, USA. <sup>15</sup>These authors contributed equally: Peter A. Smith, Michael F. T. Koehler. \*e-mail: smith.peter@gene.com; heise.christopher@gene.com

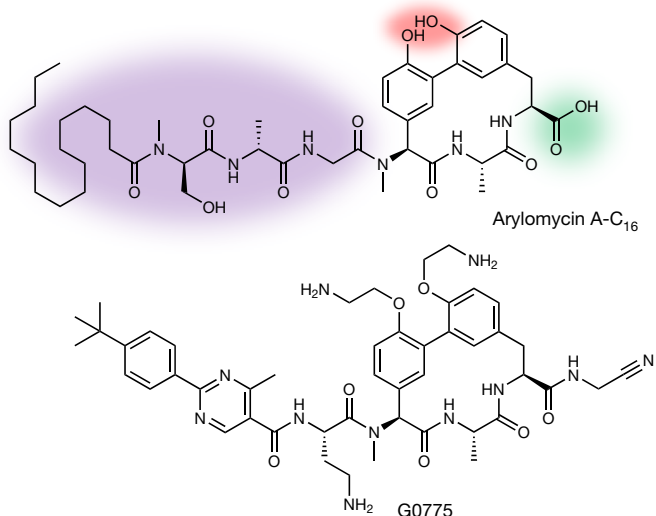


**Fig. 1 | Chemical structures of arylomycin A-C<sub>16</sub> and G0775.** Purple indicates the N-terminal lipopeptide tail, red indicates the location of phenolic oxygen modifications to the arylomycin core macrocycle and green is the site for appendage of the nitrile electrophile that covalently binds to the LepB catalytic lysine.

Gram-positive bacteria<sup>5,13,17,18</sup>. The N-terminal lipopeptide tail also interacts with the amino acid residue in LepB that reduces the binding affinity of the arylomycin natural products<sup>13</sup>, so we first searched for variants that more optimally engage this region of the Gram-negative protein. Ultimately we achieved the greatest improvement in activity by shortening the linear d-N-Me-Ser-d-Ala-Gly tripeptide in arylomycin to a single diaminobutyric acid and replacing the natural aliphatic tail with 2-(4-(*tert*-butyl)phenyl)-4-methylpyrimidine-5-carboxylic acid. This modification considerably improved the Gram-negative activity, yielding a molecule with measurable minimum inhibitory concentrations (MICs) against *E. coli* and *K. pneumoniae* (Extended Data Fig. 6). Second, we appended electrophilic warheads at the C-terminal carboxylate in an attempt to covalently bind the catalytic serine of LepB<sup>14</sup>. We identified 2-aminoacetonitrile as the optimal modification, which further improved activity against *E. coli* and *K. pneumoniae* and also imparted measurable activity against the particularly challenging bacteria *A. baumannii* and *P. aeruginosa* (Extended Data Fig. 6). Finally, inspired by modifications to the macrocyclic phenols found in natural arylomycin analogues and previous reports that phenol modifications can afford activity gains<sup>14,19</sup>, we explored the simultaneous substitution of both phenols (Fig. 1). The resulting molecule, termed G0775, is at least 500-fold more potent than arylomycin A-C<sub>16</sub> against the ESKAPE pathogens *E. coli* and *K. pneumoniae* as well as against related pathogens from the same family. Moreover, the potent activity of G0775 extends to the notoriously difficult-to-treat non-fermenting Gram-negative bacteria *P. aeruginosa* and *A. baumannii* (Table 1). Although not the primary focus of our efforts, G0775 also exhibits markedly increased potency against the important Gram-positive pathogens methicillin-resistant *S. aureus* and *Staphylococcus epidermidis*, with MICs for each less than 0.5 µg ml<sup>-1</sup> (Extended Data Fig. 6). G0775 therefore validates our hypothesis that chemical modifications can be used to expand the spectrum and potency of the natural product arylomycins to include ESKAPE pathogens and represents a new and exciting molecule that could address the need for new Gram-negative antibiotics.

## G0775 is active against MDR bacteria

After demonstrating potent activity against common laboratory strains of Gram-negative ESKAPE pathogens, we set out to determine whether G0775 circumvents the multitude of resistance mechanisms that undermine the effectiveness of currently available therapies. First, we determined the MIC of G0775 against a panel of 49 MDR clinical

**Table 1 | MIC values for arylomycin A-C<sub>16</sub> and G0775 against pathogenic Gram-negative bacteria**

Bacterial species	MIC (µg ml <sup>-1</sup> )	
	Arylomycin A-C <sub>16</sub>	G0775
<i>E. coli</i> ATCC 25922	>64	0.125
<i>K. pneumoniae</i> ATCC 43816	>64	0.125
<i>Enterobacter cloacae</i> ATCC 13407	>64	0.5
<i>Enterobacter aerogenes</i> ATCC 13408	>64	0.125
<i>Citrobacter werkmanii</i> ATCC 51114	>64	0.25
<i>Serratia marcescens</i> CDC4385-74	>64	0.5
<i>A. baumannii</i> ATCC 17978	>64	1
<i>P. aeruginosa</i> ATCC 27853	>64	2

isolates of *E. coli* and *K. pneumoniae*, which are provided by the Centers for Disease Control and Prevention (CDC) to evaluate potential new antibiotics. The panel is highly enriched for MDR pathogens, and more than half exhibited resistance to at least five of the eight clinically used antibiotics that were tested (Supplementary Table 1). In stark contrast to the approved drugs, G0775 maintains its potent activity against all 49 isolates, with 90% of the isolates exhibiting MICs of  $\leq 0.25 \mu\text{g ml}^{-1}$  (Supplementary Table 1). G0775 also remains active against 16 highly MDR strains of *A. baumannii* and 12 highly MDR strains of *P. aeruginosa* from the CDC, with 90% of the isolates exhibiting MICs of  $\leq 4 \mu\text{g ml}^{-1}$  and  $\leq 16 \mu\text{g ml}^{-1}$ , respectively. To better assess the ability of G0775 to circumvent specific resistance mechanisms, we focused on a single MDR isolate of *K. pneumoniae*, strain CDC 0106. Whole-genome sequencing of CDC 0106 revealed at least 10 chromosomally encoded and 25 plasmid-encoded genes associated with resistance to 13 classes of antibiotics (Supplementary Table 2). These genetic elements encoded by CDC 0106 confer resistance to nearly all available antibiotic classes (Table 2). Moreover, the presence of genes encoding the NDM-1 metallo beta-lactamase and the ArmA ribosomal methylase is expected to confer resistance even to new therapies recently approved for clinical use such as Vabomere and Zemdri, respectively<sup>20,21</sup>, which are new variants of known antibiotic classes. G0775 remains highly active against CDC 0106, confirming that this new class is not affected by this extensive repertoire of resistance elements.

## G0775 acts via LepB with low resistance frequency

We next set out to confirm that the improved antibacterial activity of G0775 was achieved through specific inhibition of LepB and not by means of off-target or secondary mechanisms. We first created a strain in which LepB expression levels are controlled by the concentration of arabinose in the growth medium (Extended Data Fig. 1), and found that low levels of LepB expression resulted in a 16-fold increase in susceptibility relative to wild-type cells, whereas high levels of LepB expression decrease susceptibility by eightfold (Extended Data Table 1). Next, we explored the rate at which G0775 kills bacteria. Genetic depletion of LepB in *E. coli* leads to time-dependent cell death<sup>22</sup>, and G0775 likewise causes time-dependent killing at a similar rate, ultimately reducing the number of viable bacteria by more than six orders of magnitude after 24 h (Extended Data Fig. 1). The target titration and time-kill data are consistent with G0775 acting via LepB inhibition. To unequivocally confirm this, we assessed the ability of diverse Gram-negative ESKAPE pathogens to spontaneously evolve resistance to G0775. As expected for an inhibitor that targets a single gene product<sup>23</sup>, resistant mutants were isolated at a moderate frequency in the presence of a low concentration of G0775 (4× MIC). When selections were performed with a higher concentration of G0775 (8× MIC), the frequency of resistance was below the limit of detection for *K. pneumoniae* and *A. baumannii*. At 16× MIC, the frequency of resistance for *E. coli* and *P. aeruginosa* decreased to less than  $10^{-10}$  (Fig. 2a). Targeted and whole-genome sequencing of G0775-resistant *E. coli* mutants revealed that resistance-conferring mutations in all but four isolates were found

**Table 2 | MIC values for G0775 and antibiotics from diverse classes against MDR *K. pneumoniae* CDC 0106**

Class	Antibiotic	MIC ( $\mu\text{g ml}^{-1}$ )
Cephalosporin/ $\beta$ -lactamase inhibitor	Ceftazidime/avibactam	>64
Aminoglycoside	Gentamicin	>64
Fluoroquinolone	Levofloxacin	>64
Carbapenem	Meropenem	>64
Polymyxin	Colistin	16
Tetracycline	Tigecycline	2
Arylomycin	G0775	0.5

within the substrate-binding groove of LepB, which confirms that the whole-cell activity of G0775 is on target. Encouragingly, these mutations reduce susceptibility to G0775 by only 4- to 16-fold (Extended Data Table 2), which is consistent with the marked decrease in resistance frequencies in the presence of higher drug concentrations. The remaining four isolates each contained a missense mutation (N282Y) in *acrB*, a gene that encodes an efflux pump; this may increase the affinity of this efflux system for G0775. Deletion of the AcrB or TolC efflux pumps in wild-type *E. coli* had no effect on the potency of G0775, which suggests that AcrB(N282Y) is a gain-of-function mutation and demonstrates that the native *E. coli* efflux systems do not considerably affect the activity of G0775 (Extended Data Table 1). Taken together, these results demonstrate that G0775 kills Gram-negative bacteria by means of LepB inhibition, and that spontaneous resistance to G0775 occurs primarily via on-target mutations that provide only modest decreases in susceptibility.

### G0775 binds to LepB in an unprecedented manner

To test the hypothesis that resistance-conferring *lepB* mutations alter residues that directly contact the inhibitor, we solved the co-crystal structure of LepB in complex with G0775 to 2.4 Å resolution. By mapping the selected G0775-resistant mutations onto the *E. coli* LepB crystal structure, we confirmed that these mutations lie within the substrate-binding groove and closely overlay the G0775 binding site (Fig. 2b). Indeed, all of the resistance-conferring mutations lie within 4.5 Å of the bound inhibitor and, in total, mutations were identified in 8 of the 20 residues that contact G0775. Overall the LepB–G0775 structure reveals that the macrocyclic core and the backbone amide heteroatoms of the inhibitor bind in an almost identical manner to that previously observed in structures of arylomycins bound to LepB<sup>15,16</sup>, despite the addition of an electrophilic warhead to the C terminus (Extended Data Fig. 2). Notably, the aminoacetonitrile warhead on G0775 does not engage the catalytic serine (S91) as we had expected, but instead reacts with the nitrogen of the catalytic lysine (K146) (Fig. 3a, Extended Data Fig. 4). This is consistent with the formation of a covalent amidine through direct nucleophilic attack of the electrophilic nitrile by the catalytic lysine, which is an inversion of the typical roles of the active-site dyad (Extended Data Fig. 3) and, to our knowledge, is the first report of amidine formation between an inhibitor and its target protein. To confirm the nature of this covalent interaction, we incubated LepB with an excess of G0775 overnight, digested with trypsin and subjected the digest to analysis by liquid chromatography coupled with mass spectrometry (LC–MS) (Fig. 3b). The resulting fragments confirm the formation of an adduct of the expected molecular weight between G0775 and a LDYIKR peptide fragment that includes the catalytic residue K146. This mechanism of covalent protease inhibition is—to our knowledge—unique to our molecules, and adds a new tool to the rapidly expanding field of covalent enzyme inhibitors<sup>24</sup>. Detailed kinetic enzymology studies of full-length LepB embedded in a detergent micelle were performed to quantify the rate of covalent-bond formation with the catalytic lysine. The data indicate very tight reversible binding of the molecule into the substrate-binding pocket ( $K_I = 0.44 \text{ nM}$ ) followed by irreversible inactivation ( $k_{\text{inact}} = 0.0007 \text{ s}^{-1}$ ;  $k_{\text{inact}}/K_I = 1,590,909 \text{ M}^{-1} \text{ s}^{-1}$ ) (Fig. 3c), which confirms the very high affinity of G0775 for LepB.

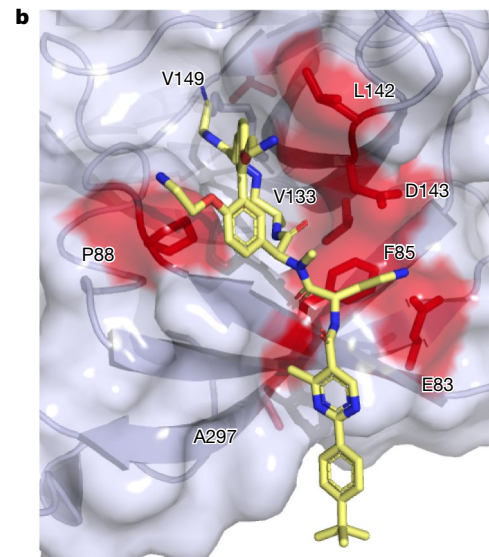
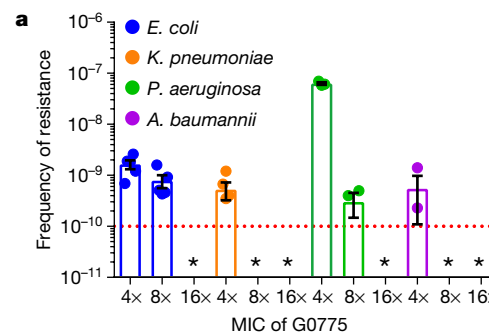


**Fig. 2 | Resistance to G0775.** **a**, Frequencies of resistance of *E. coli* ATCC 25922, *K. pneumoniae* 43816, *P. aeruginosa* PAO1 and *A. baumannii* ATCC 17978 to G0775 at 4, 8 and 16 times the respective MIC of each strain. The limit of detection ( $10^{-10}$ ) is marked by the red dotted line, with asterisks representing data points that fall below the limit. Data shown for *E. coli* and *K. pneumoniae* are an average of five independent experiments, whereas data shown for *P. aeruginosa* and *A. baumannii* are an average of three independent experiments. Error bars represent s.d. **b**, LepB target mutations mapped onto the G0775–LepB crystal structure. Mutants were spontaneously generated in *E. coli* ATCC 25922 by overnight plating on G0775 at 4× MIC and are indicated in red. G0775 is shown in stick representation.

### G0775 access to LepB is porin-independent

To inhibit LepB, which is localized on the inner membrane, G0775 must first cross the outer membrane. As a surrogate for the efficiency of outer membrane penetration, we determined the potency of G0775 against a hyperpermeable *E. coli* mutant, *lptD4213* (*imp*), which exhibits a defect in the outer membrane biogenesis pathway and is highly sensitive to both lipophilic and large hydrophilic antibiotics that are otherwise excluded by the outer membrane<sup>25</sup>. The *imp* mutation renders *E. coli* 32-fold more sensitive to G0775, and EDTA-mediated chelation (EDTA, ethylenediaminetetraacetic acid) of the divalent cations that are necessary to maintain the stability of the outer membrane results in a similar increase in potency (Extended Data Table 1). These data suggest that, despite its high molecular mass and high polarity, G0775 penetrates the outer membrane with reasonable efficiency. The majority of polar antibiotics that cross the outer membrane do so through open, water-filled channels called porins. However, deletion of OmpC or OmpF, the primary porins in *E. coli*, either individually or in combination has no effect on the potency of G0775 (Extended Data Table 1). Although it remains possible that other porins contribute to outer membrane penetration, porin mutations were never identified in resistance studies and the high molecular mass of G0775 (890 g mol<sup>-1</sup>)

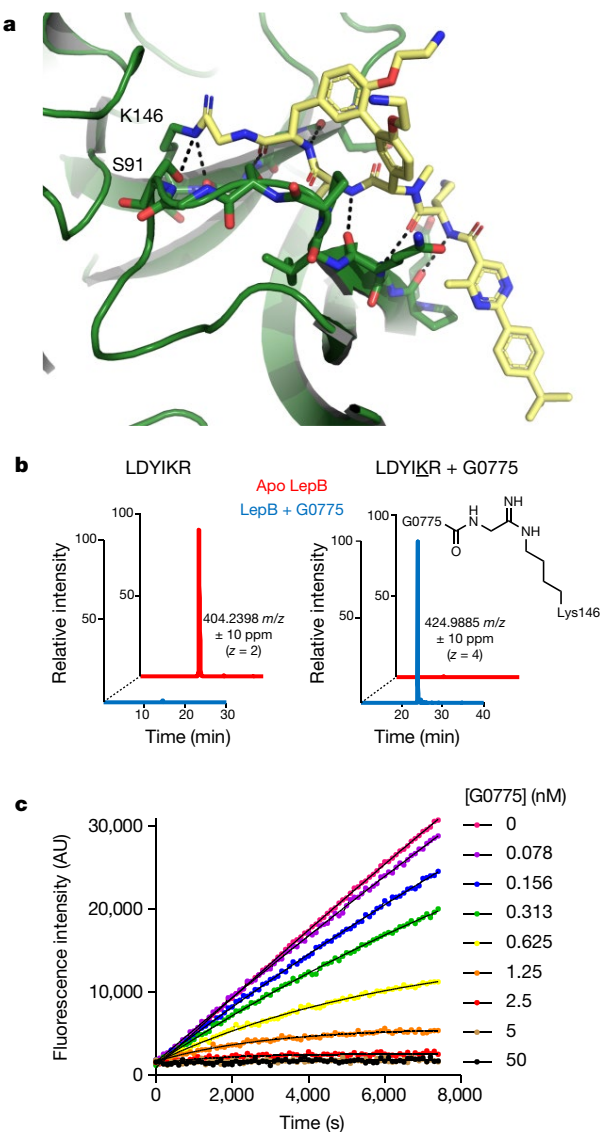


**Fig. 3 | G0775 binds the LepB protease domain to form an irreversible covalent bond with catalytic lysine 146.** **a**, Crystal structure of the protease domain of LepB at 2.4 Å resolution, with G0775 represented as sticks covalently bound to lysine 146. **b**, LC–MS detection of LDYIKR LepB peptide fragment after tryptic digest following the incubation of LepB with G0775. The unmodified peptide (red) is detected only in the absence of incubation with G0775, whereas the LDYIKR–G0775 peptide adduct (blue) is detected only after the incubation of LepB with G0775. This study was performed twice with similar results. **c**, LepB kinetic enzyme assays in the presence of the indicated concentrations of G0775. The nonlinear inactivation curves indicate time-dependent inhibition consistent with covalent bond formation.  $K_{inact}$  ( $0.0007 \pm 0.0002 \text{ s}^{-1}$ ) and  $K_1$  ( $0.44 \pm 0.15 \text{ M}^{-1} \text{ s}^{-1}$ ) were measured from three independent experiments and the data points shown are averages of four replicates from a single experiment. AU, arbitrary units.

is above the range typically considered compatible with porin-mediated entry<sup>26</sup> (Extended Data Fig. 5c). An alternative entry mechanism, whereby compounds bind to and destabilize the outer membrane, is termed ‘self-promoted uptake’, and the presence of positively charged groups can facilitate this process<sup>27</sup>. An analysis of the activity of more than 1,000 distinct arylomycin analogues against wild-type and outer-membrane-permeable *E. coli* suggests a modest beneficial effect of amines on the outer membrane penetrance of arylomycins (Extended Data Fig. 5a, b). To assess more directly the contribution of positive charge to the outer membrane penetrance of G0775, we synthesized neutral analogues that lacked all three primary amines (Extended Data

Figs. 5b, 6). These analogues remain active against wild-type *E. coli*, which demonstrates that amines are not essential for outer membrane penetrance; however, consistent with our global analysis, the efficiency of these analogues in penetrating the outer membrane, as measured in our shift assay, is eightfold lower than that of G0775. Notably, removal of the amines from G0775 reduces potency against both outer-membrane-permeable *E. coli* and against the Gram-positive bacteria *S. aureus* by 32- to 64-fold, which is consistent with an important role for the amines in the intrinsic potency of G0775. Taken together, these data suggest that G0775 and related analogues penetrate the outer membrane through a porin-independent mechanism, which is likely to be a form of self-promoted uptake that is enhanced by the presence of positive charge.

### Efficacy of G0775 *in vivo* against ESKAPE pathogens

The potent *in vitro* activity of G0775 in the presence of 50% serum or 1% lung surfactant (Extended Data Table 1) suggested that this antibiotic could be used to treat serious systemic and pulmonary infections. To confirm this, we tested G0775 in several pre-clinical infection models with different pathogenic Gram-negative bacteria. First, we evaluated the *in vivo* efficacy of G0775 in the murine neutropenic thigh infection model, which assesses intrinsic antibacterial activity independent from the innate immune system and has established translatability to efficacy in humans. G0775 demonstrates potent bactericidal activity (>2-log decrease in colony-forming units) against the *E. coli* strain ATCC 25922 and the *K. pneumoniae* strain ATCC 43816 at 1 mg kg<sup>-1</sup> and 5 mg kg<sup>-1</sup>, respectively (Fig. 4a, Extended Data Fig. 7). Next, we tested G0775 against *P. aeruginosa* ATCC 27853 and *A. baumannii* ATCC 17978 in the same neutropenic thigh model. A higher concentration of G0775 was required for efficacy, consistent with the higher MIC values for these pathogens (Fig. 4a). Third, we used a lung-infection model to assess the activity of G0775 against an MDR bacterial pulmonary infection. Using the MDR CDC 0106 (Table 2) as the challenge pathogen, G0775 was bacteriostatic at 2 mg kg<sup>-1</sup> and bactericidal at 20 mg kg<sup>-1</sup> (Fig. 4b). These results confirm that this new class of antibiotic is able to overcome all of the resistance mechanisms inherent to CDC 0106 *in vitro* and *in vivo*. Finally, we examined the ability of G0775 to protect mice from a lethal challenge of *K. pneumoniae* Z strain ATCC 43816 in a mucin peritonitis model. G0775 effected a dose-dependent increase in survival, with 5 mg kg<sup>-1</sup> delivered twice on day 0 of the infection able to maintain full viability of mice until 84 h (Fig. 4c). Taken together, these *in vivo* efficacy data, combined with a lack of mammalian cell toxicity (Extended Data Table 3), demonstrate the potential of G0775 to treat several types of infections caused by a variety of wild-type and MDR Gram-negative bacteria.

### Discussion

The growth in MDR bacterial infections is a serious risk to global health, and most antibacterial discovery efforts focus on reinvigorating existing classes of clinically approved antibiotics by means of chemical modification. Although this approach has been critical and effective, the resulting molecules are eventually subject to the same types of resistance mechanisms, which evolve and disseminate in response to previously used members of the class. By contrast, owing to its novel mechanism of action, G0775 bypasses existing resistance mechanisms and exhibits potent *in vitro* and *in vivo* activity against MDR Gram-negative bacteria, including extremely drug-resistant strains such as the clinical isolate CDC 0106.

The potent whole-cell activity of G0775 is the product of excellent affinity for its target, the avoidance of efflux and its relatively efficient outer membrane penetration. Ultimately, the ability of G0775 to cross the outer membrane is surprising, given that its physicochemical properties are quite distinct from those of other approved Gram-negative antibiotics<sup>10</sup>. This disconnect probably reflects the fact that most Gram-negative antibiotics cross the outer membrane through porins, whereas G0775 uses a porin-independent mechanism. Although considerable advances have been made in our understanding of porin-mediated

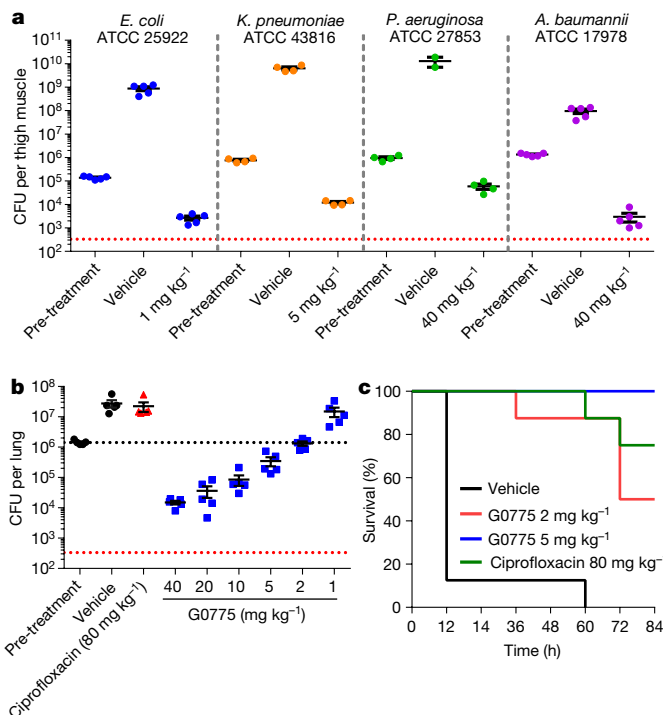


**Fig. 4 | In vivo efficacy of G0775.** **a**, Thigh infections initiated in neutropenic mice with the indicated Gram-negative bacterial species were treated with G0775 ( $n=5$  mice for *E. coli* and *A. baumannii*;  $n=4$  mice for *K. pneumoniae* and *P. aeruginosa*) or vehicle ( $n=2$  mice for *P. aeruginosa*,  $n=4$  mice for *K. pneumoniae*,  $n=5$  mice for *E. coli* and *A. baumannii*), and the bacterial burden was quantified 20 h after infection. G0775 was delivered subcutaneously twice during the infection period at 2 and 11 h post-infection at the indicated dose. **b**, Dose-dependent antibacterial activity of G0775 against a bacterial infection established by the MDR *K. pneumoniae* clinical isolate CDC 0106 in the lungs of neutropenic mice ( $n=5$ ). G0775 was delivered subcutaneously twice during the 20-h infection period at 2 and 11 h after the initiation of infection. The centre bars for **a** and **b** represent the mean, error bars represent s.e.m. and dotted red lines represent the limit of determination of bacterial colony forming units (CFU). **c**, Kaplan–Meier survival analysis of mice after peritoneal infection with *K. pneumoniae* ATCC 43816. G0775 was delivered subcutaneously twice on day zero at 2 and 11 h after the initiation of infection, and the viability of mice ( $n=8$ ) was monitored until 84 h.

entry<sup>11,12</sup>—culminating in prospective guidelines for improving the porin-mediated accumulation of compounds in Gram-negative bacteria<sup>28</sup>—considerably less is known about the features that enable efficient porin-independent penetration of the outer membrane<sup>29</sup>. Polymyxins, the polycationic antibiotics of last resort, cross the outer membrane by means of self-promoted uptake owing to their positive charge<sup>27</sup>, and resistance readily emerges through alterations to the outer membrane that block this process<sup>30</sup>. Importantly, G0775 remains active against polymyxin-resistant isolates, and our data show that positive charge is beneficial to, but not essential for, the penetration of arylomycin through the outer membrane. Indeed other large, polar, non-charged inhibitors of periplasmic targets—such as globomycin—have Gram-negative antibacterial activity and exhibit relatively efficient penetration of the outer membrane<sup>31</sup>. A better understanding of the features that enable efficient porin-independent penetration of the outer membrane may help to inform the design of new Gram-negative antibiotics with properties that are distinct from current classes, and our ongoing studies of G0775 and related molecules may help to elucidate these features.

In summary, the broad spectrum and potent activity of G0775, combined with its low vulnerability to spontaneous resistance and excellent preclinical efficacy, suggest that optimized arylomycin analogues may represent a much-needed new class of Gram-negative antibiotic. Such a new mechanistic class of antibiotic has the potential to reset the clock

in the ongoing arms race with pathogenic bacteria and help to postpone the prospect of a return to the pre-antibiotic era.

## Reporting summary

Further information on experimental design is available in the Nature Research Reporting Summary linked to this paper.

## Data availability

The sequence reported in this paper has been deposited in the GenBank database, [www.ncbi.nlm.nih.gov/genbank](http://www.ncbi.nlm.nih.gov/genbank) (accession numbers CP022611–CP022613). G0775, G3031, G8126 and G6850 are unique molecules proprietary to Genentech that are readily available on request. The authors declare that all other data supporting the findings of this study are available from the authors and/or included with the manuscript as Source Data (efficacy studies) or as Supplementary Information.

## Online content

Any methods, additional references, Nature Research reporting summaries, source data, statements of data availability and associated accession codes are available at <https://doi.org/10.1038/s41586-018-0483-6>.

Received: 6 October 2017; Accepted: 26 June 2018;

Published online 12 September 2018.

- Ventola, C. L. The antibiotic resistance crisis part 1: causes and threats. *P&T* **40**, 277–283 (2015).
- Rice, L. B. Federal funding for the study of antimicrobial resistance in nosocomial pathogens: no ESKAPE. *J. Infect. Dis.* **197**, 1079–1081 (2008).
- Schiranna, J. et al. Arylomycins A and B, new biaryl-bridged lipopeptide antibiotics produced by *Streptomyces* sp. Tü 6075. I. Taxonomy, fermentation, isolation and biological activities. *J. Antibiot. (Tokyo)* **55**, 565–570 (2002).
- Kulanthaivel, P. et al. Novel lipoglycopeptides as inhibitors of bacterial signal peptidase I. *J. Biol. Chem.* **279**, 36250–36258 (2004).
- Smith, P. A., Powers, M. E., Roberts, T. C. & Romesberg, F. E. In vitro activities of arylomycin natural-product antibiotics against *Staphylococcus epidermidis* and other coagulase-negative staphylococci. *Antimicrob. Agents Chemother.* **55**, 1130–1134 (2011).
- Paetzel, M., Dalbey, R. E. & Strynadka, N. C. The structure and mechanism of bacterial type I signal peptidases. A novel antibiotic target. *Pharmacol. Ther.* **87**, 27–49 (2000).
- Smith, R. C. & Anné, J. Bacterial type I signal peptidases as antibiotic targets. *Future Microbiol.* **6**, 1279–1296 (2011).
- Bruton, G. et al. Lipopeptide substrates for SpsB, the *Staphylococcus aureus* type I signal peptidase: design, conformation and conversion to  $\alpha$ -ketoamide inhibitors. *Eur. J. Med. Chem.* **38**, 351–356 (2003).
- Payne, D. J., Gwynn, M. N., Holmes, D. J. & Pompliano, D. L. Drugs for bad bugs: confronting the challenges of antibacterial discovery. *Nat. Rev. Drug Discov.* **6**, 29–40 (2007).
- O’Shea, R. & Moser, H. E. Physicochemical properties of antibacterial compounds: implications for drug discovery. *J. Med. Chem.* **51**, 2871–2878 (2008).
- Nikaido, H. Molecular basis of bacterial outer membrane permeability revisited. *Microbiol. Mol. Biol. Rev.* **67**, 593–656 (2003).
- Brown, D. G., May-Dracka, T. L., Gagnon, M. M. & Tommasi, R. Trends and exceptions of physical properties on antibacterial activity for Gram-positive and Gram-negative pathogens. *J. Med. Chem.* **57**, 10144–10161 (2014).
- Smith, P. A., Roberts, T. C. & Romesberg, F. E. Broad-spectrum antibiotic activity of the arylomycin natural products is masked by natural target mutations. *Chem. Biol.* **17**, 1223–1231 (2010).
- Liu, J., Smith, P. A., Steed, D. B. & Romesberg, F. Efforts toward broadening the spectrum of arylomycin antibiotic activity. *Bioorg. Med. Chem. Lett.* **23**, 5654–5659 (2013).
- Luo, C., Roussel, P., Dreier, J., Page, M. G. P. & Paetzel, M. Crystallographic analysis of bacterial signal peptidase in ternary complex with arylomycin A2 and a  $\beta$ -sultam inhibitor. *Biochemistry* **48**, 8976–8984 (2009).
- Liu, J. et al. Synthesis and characterization of the arylomycin lipoglycopeptide antibiotics and the crystallographic analysis of their complex with signal peptidase. *J. Am. Chem. Soc.* **133**, 17869–17877 (2011).
- Roberts, T. C., Schallenger, M. A., Liu, J., Smith, P. A. & Romesberg, F. E. Initial efforts toward the optimization of arylomycins for antibiotic activity. *J. Med. Chem.* **54**, 4954–4963 (2011).
- Therien, A. G. et al. Broadening the spectrum of  $\beta$ -lactam antibiotics through inhibition of signal peptidase type I. *Antimicrob. Agents Chemother.* **56**, 4662–4670 (2012).
- Peters, D. S., Romesberg, F. E. & Baran, P. S. Scalable access to arylomycins via C–H functionalization logic. *J. Am. Chem. Soc.* **140**, 2072–2075 (2018).
- Castanheira, M., Huband, M. D., Mendes, R. E. & Flamm, R. K. Meropenem-vaborbactam tested against contemporary gram-negative isolates collected worldwide during 2014, including carbapenem-resistant, KPC-producing, multidrug-resistant, and extensively drug-resistant *Enterobacteriaceae*. *Antimicrob. Agents Chemother.* <https://doi.org/10.1128/AAC.00567-17> (2017).
- Endimiani, A. et al. ACHN-490, a neoglycoside with potent *in vitro* activity against multidrug-resistant *Klebsiella pneumoniae* isolates. *Antimicrob. Agents Chemother.* **53**, 4504–4507 (2009).

22. Lüke, I., Handford, J. I., Palmer, T. & Sargent, F. Proteolytic processing of *Escherichia coli* twin-arginine signal peptides by LepB. *Arch. Microbiol.* **191**, 919–925 (2009).
23. Silver, L. L. Multi-targeting by monotherapeutic antibacterials. *Nat. Rev. Drug Discov.* **6**, 41–55 (2007).
24. Singh, J., Petter, R. C., Baillie, T. A. & Whitty, A. The resurgence of covalent drugs. *Nat. Rev. Drug Discov.* **10**, 307–317 (2011).
25. Sampson, B. A., Misra, R. & Benson, S. A. Identification and characterization of a new gene of *Escherichia coli* K-12 involved in outer membrane permeability. *Genetics* **122**, 491–501 (1989).
26. Silver, L. L. Challenges of antibacterial discovery. *Clin. Microbiol. Rev.* **24**, 71–109 (2011).
27. Hancock, R. E. & Bell, A. Antibiotic uptake into Gram-negative bacteria. *Eur. J. Clin. Microbiol. Infect. Dis.* **7**, 713–720 (1988).
28. Richter, M. F. et al. Predictive compound accumulation rules yield a broad-spectrum antibiotic. *Nature* **545**, 299–304 (2017).
29. Richter, M. F. & Hergenrother, P. J. The challenge of converting Gram-positive-only compounds into broad-spectrum antibiotics. *Ann. NY Acad. Sci.* **24**, 71 (2018).
30. Raetz, C. R. H., Reynolds, C. M., Trent, M. S. & Bishop, R. E. Lipid A modification systems in Gram-negative bacteria. *Annu. Rev. Biochem.* **76**, 295–329 (2007).
31. Kiho, T. et al. Structure–activity relationships of globomycin analogues as antibiotics. *Bioorg. Med. Chem.* **12**, 337–361 (2004).

**Acknowledgements** We thank Confluence Discovery Technologies for running the enzymatic inactivation studies and WuXi Shanghai for determining MIC values to support the chemistry effort. We thank C. Peng, H. La, J. Z. Chen, F. Ma, X. Liang, S. Ubhayakar and the protein expression group from Genentech for supporting the research efforts required to discover G0775, J. Guillory for performing the whole-genome sequencing on CDC 0106, and B. Sellers for performing property calculations on synthesized compounds.

**Reviewer information** *Nature* thanks E. Brown, P. Hergenrother, T. Maier and the other anonymous reviewer(s) for their contribution to the peer review of this work.

**Author contributions** P.A.S., M.F.T.K., Yu.C., M.R.D., M.X., M.W.T. and C.E.H. conceived the study and managed the execution of experiments. H.S.G. and P.A.S. performed all the microbiology experiments. D.Y., J.K., S.P., M.X. and H.Z. performed all *in vivo* efficacy studies. J.M. and L.R. performed all crystallographic experiments. W.P. performed the proteomics experiments. C.E.H. and J.G.Q. performed enzymology experiments. M.F.T.K., P.A.S., Yo.C., J.J.C., T.C.R., R.I.H., P.P., J.B.S., J.W. and Z.Y. designed and synthesized the molecules. E.S. performed the whole-genome sequencing. P.A.S., M.F.T.K. and C.E.H. wrote the manuscript with input from all authors.

**Competing interests** P.A.S., M.F.T.K., Yo.C., J.J.C., R.I.H., P.P., T.C.R., J.B.S. and Z.Y. are listed as inventors on the pending patent application WO2017084630, which covers the molecules G0775, G6850, G3031 and G8126. P.A.S., M.F.T.K., Yu.C., M.R.D., M.X., M.W.T., H.S.G., D.Y., J.K., S.P., H.Z., J.M., L.R., W.P., J.G.Q., J.J.C. and C.E.H. declare active employment by Genentech at the time of submission.

#### Additional information

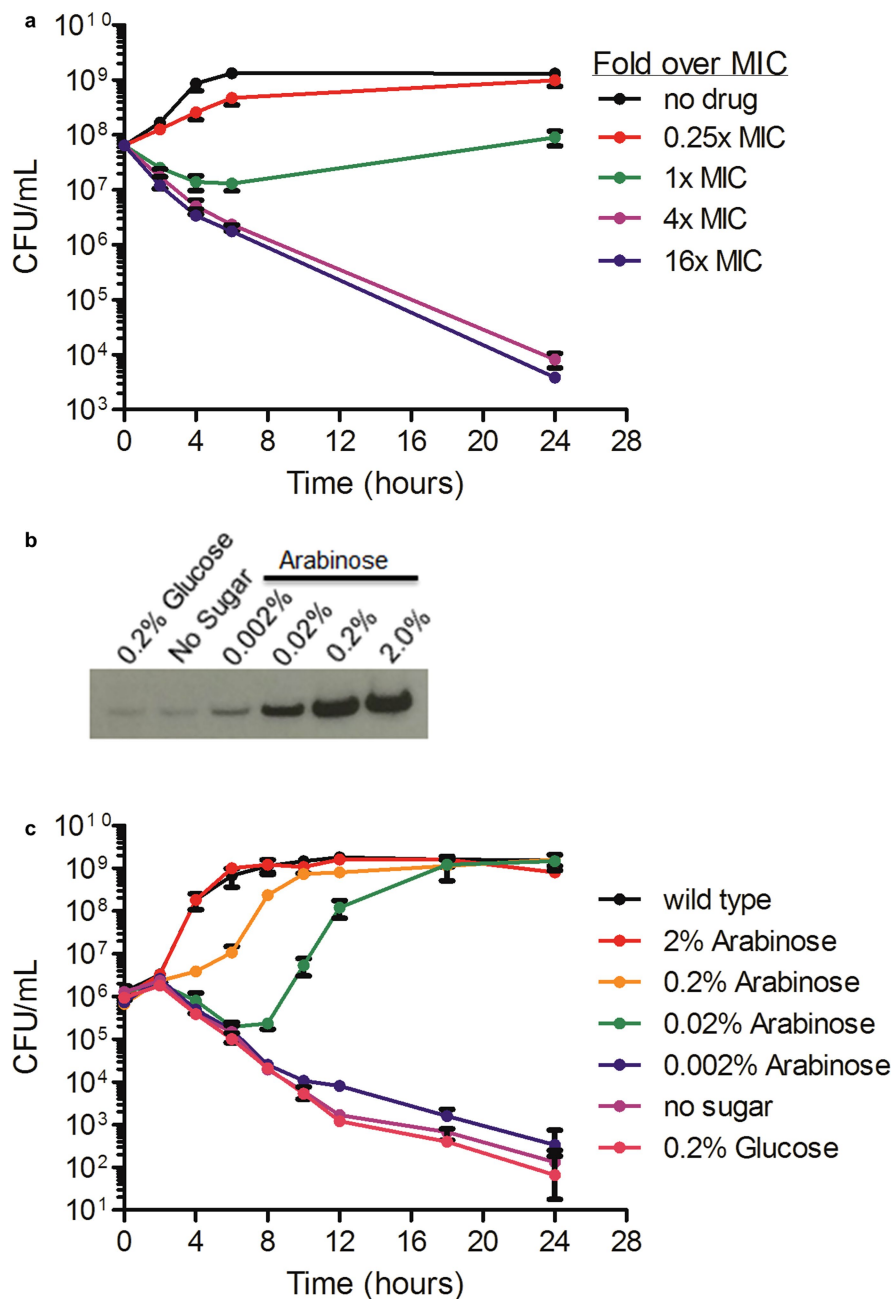
**Extended data** is available for this paper at <https://doi.org/10.1038/s41586-018-0483-6>.

**Supplementary information** is available for this paper at <https://doi.org/10.1038/s41586-018-0483-6>.

**Reprints and permissions information** is available at <http://www.nature.com/reprints>.

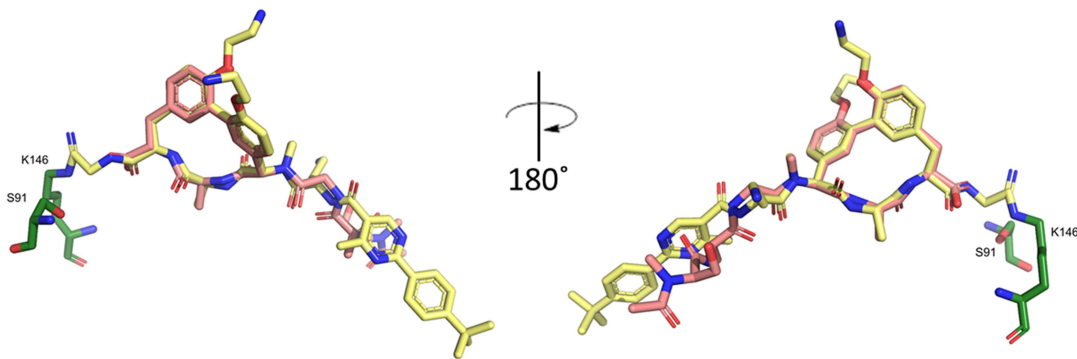
**Correspondence and requests for materials** should be addressed to P.A.S. or C.E.H.

**Publisher's note:** Springer Nature remains neutral with regard to jurisdictional claims in published maps and institutional affiliations.



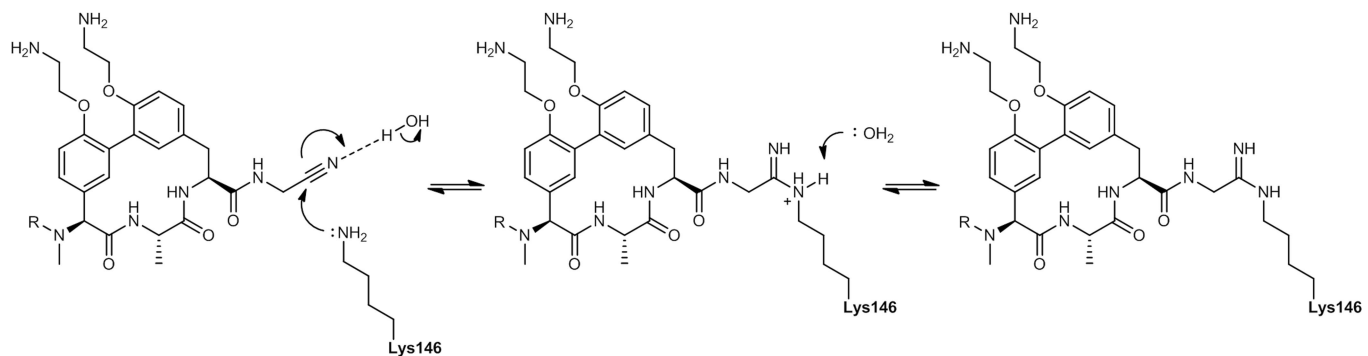
**Extended Data Fig. 1 | Growth rates of *E. coli* during treatment with G0775 or when LepB expression levels are modulated.** **a**, Time-kill data of *E. coli* ATCC 25922 when treated with G0775 at 0.25, 1, 4 and 16 times the measured MIC of  $0.125 \mu\text{g ml}^{-1}$ . The data is an average of three independent experiments with error bars representing s.d. **b**, Western blot of V5-epitope-tagged LepB from an arabinose-inducible conditional LepB

strain (*E. coli* UPEC CFT073) grown in the indicated sugar concentrations. This experiment was performed once. **c**, Growth-curve analysis of the same conditional LepB strain grown in the indicated sugar concentrations. Data is an average of triplicate data points with error bars representing s.d. The graph is a representative of three independent experiments.

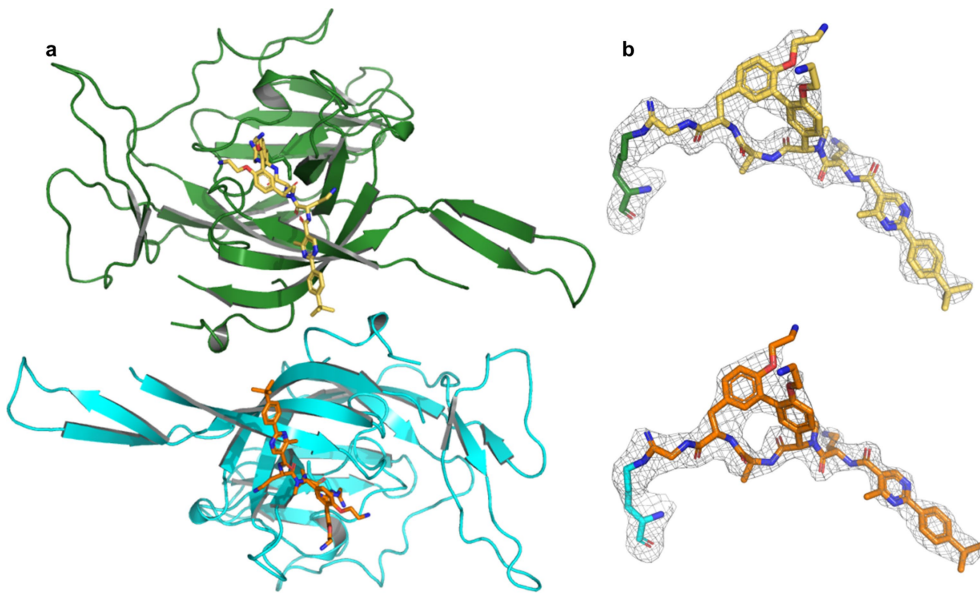


**Extended Data Fig. 2 | Overlay of LepB–G0775 and LepB–arylomycin A2 (PDB ID: 1T7D).** Comparison of G0775 (coloured yellow) and arylomycin (coloured pink). The catalytic lysine 146 is covalently bound to the nitrile warhead, while the serine 91 nucleophile remains unbound. For

simplicity, the LepB protein has been removed from each co-structure. The comparison indicates that the macrocyclic core of G0775 maintains high similarity to the parent arylomycin macrocycle, and makes very similar interactions with the protein.

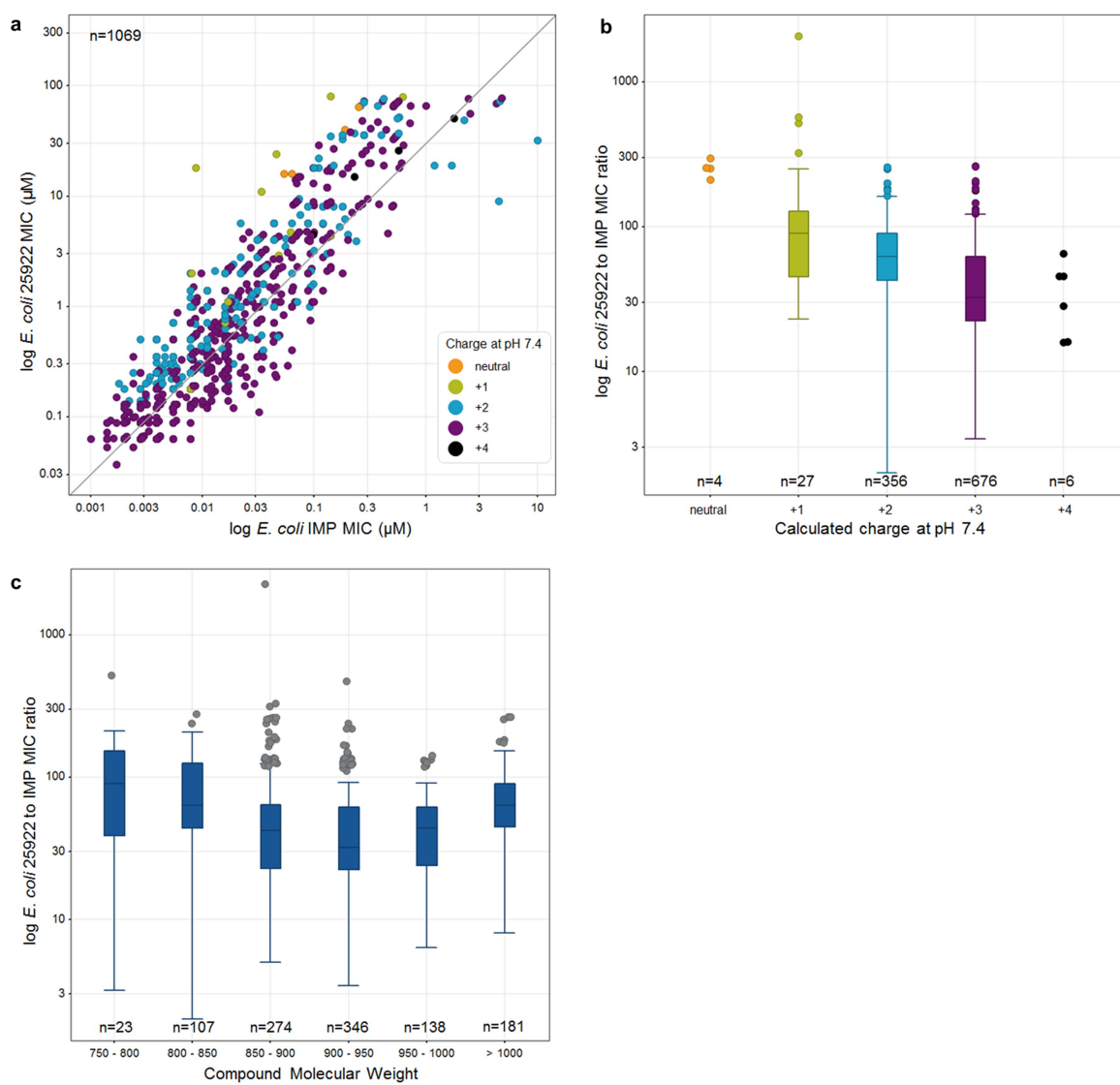


**Extended Data Fig. 3 | Proposed mechanism of covalent amidine-bond formation between G0775 nitrile and lysine 146.** The general base (lysine 146) involved in substrate proteolysis functions instead as a nucleophile to attack the nitrile warhead.



**Extended Data Fig. 4 | Details of the asymmetric unit and the electron density of the LepB–G0775 complex.** **a**, The LepB–G0775 complex crystallized in space group *I*4 with two molecules in the asymmetric unit. Chain A is coloured green, with the inhibitor shown as sticks and its carbon atoms in wheat; chain B is coloured cyan, with the inhibitor shown

as sticks and its carbon atoms coloured orange. Lattice contacts across symmetry-related molecules are not shown for clarity. **b**,  $mF_o - DF_c$  omit maps for each inhibitor molecule in the asymmetric unit are shown as grey mesh contoured at  $3\sigma$ .

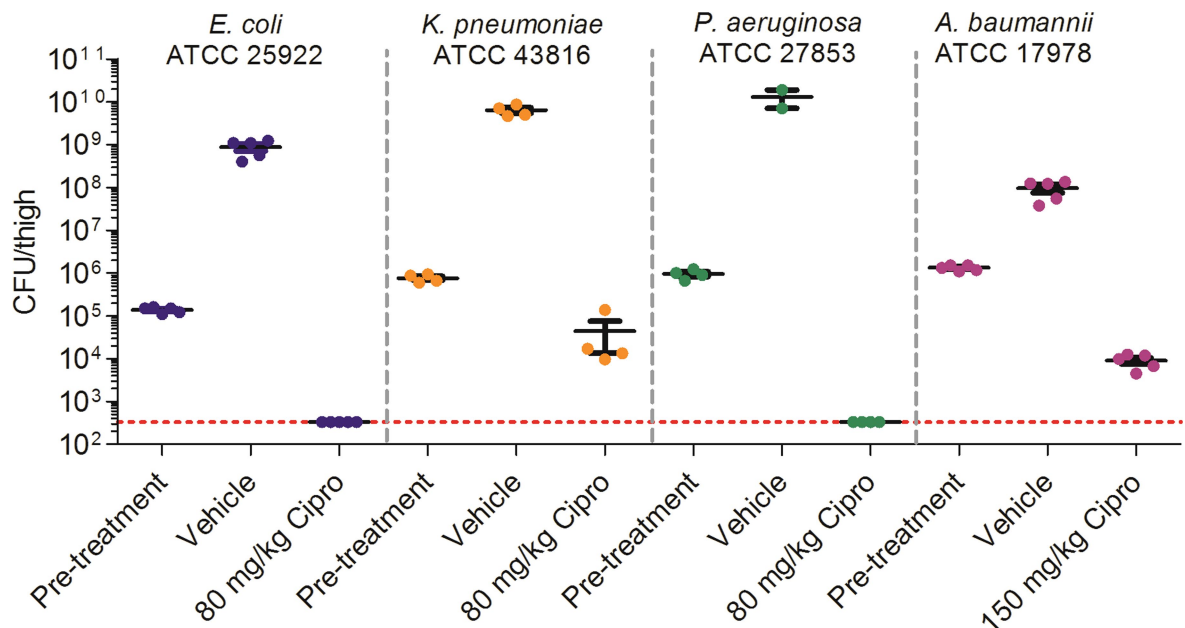


**Extended Data Fig. 5 | Analysis of Gram-negative outer membrane permeability for 1,069 arylomycin analogues.** **a**, MIC values of test compounds against *E. coli* ATCC 25922 and the outer-membrane-permeabilized *E. coli* IMP strain in the K-12 background show a consistent shift across nearly three orders of magnitude of activity. A grey line indicates a 30-fold shift in activity, and the points are coloured by the charge calculated to be the predominant species in solution at pH 7.4. Charges were calculated using MoKa 2.6.6. MIC values were measured in duplicate at a minimum, and the geometric mean was plotted. **b**, Box-and-whisker plot illustrating the IMP:25922 ratio of MIC values, for each

indicated charge state from neutral to +4 charged compounds. **c**, Box-and-whisker plots showing the IMP:25922 ratio of MIC values with the compounds subdivided by molecular weight. For **b** and **c**, the central horizontal line indicates the median value for each group, and the box ends indicate the first and third quartiles in each group. The whiskers correspond to the highest non-outlier points in each group. Outliers are defined as the points outside the median value  $\pm 1.5$ -fold the difference between the third quartile and first quartile. Outlier points are plotted individually.

	Gram outer membrane	<i>negative</i>	<i>negative</i>	<i>negative</i>	<i>negative</i>	<i>positive</i>	<i>positive</i>	<i>positive</i>	<i>positive</i>
Species	<i>E. coli</i>	<i>E. coli</i>	<i>A. bau</i>	<i>P. aer</i>	<i>S. epid</i>	<i>S. aure</i>	<i>S. pneu</i>	<i>E. faec</i>	
Strain	K12 IptD(4213)	ATCC 25922	ATCC 17978	ATCC 27853	RP62A	USA300	ATCC 49619	ATCC 29212	
	Arylomycin A-C16	16	>64	>128	>64	0.25	32	>64	>64
	G3031	0.125	8	>64	>64	>64	4	>64	>64
	G8126	0.25	32	>64	>64	4	2	>64	>64
	G6850	0.03	4	8	32	2	0.5	>64	64
	G0775	0.008	0.125	1	2	0.25	0.06	64	64

**Extended Data Fig. 6 | Chemical structures and biological activities of molecules along the optimization pathway from arylomycin A-C<sub>16</sub> to G0775.** MICs reported are in  $\mu\text{g ml}^{-1}$  units.



**Extended Data Fig. 7 | In vivo efficacy of ciprofloxacin.** Thigh infections initiated in neutropenic mice with the indicated Gram-negative bacterial species were treated with ciprofloxacin (Cipro) ( $n = 5$  mice for *E. coli* and *A. baumannii*;  $n = 4$  mice for *K. pneumoniae* and *P. aeruginosa*) or vehicle ( $n = 2$  mice for *P. aeruginosa*,  $n = 4$  mice for *K. pneumoniae*,  $n = 5$  mice for *E. coli* and *A. baumannii*), and bacterial burden was quantified 20 h

after infection. Ciprofloxacin was delivered subcutaneously once during the infection period, 2 h post-infection at the indicated dose. The pre-treatment and vehicle groups are identical to those shown in Fig. 4a, as these data were generated in the same studies. Broken red lines represent the limit of bacterial CFU determination, and the centre measure represents the mean with error bars representing s.e.m.

**Extended Data Table 1 | MIC values of G0775 measured against *E. coli* K-12 MG1655, uropathogenic *E. coli* (UPEC) and isogenic matched strains with the indicated genetic or pharmacological manipulation**

Strain	Phenotype	G0775 MIC (μg/ml)
MG1655 WT	WT	0.125
MG1655 ΔacrB	Efflux null	0.125
MG1655 ΔtolC	Efflux null	0.063
MG1655 ΔompC	Porin deficient	0.125
MG1655 ΔompF	Porin deficient	0.125
MG1655 ΔompC, ΔompF	Doubly porin deficient	0.125
MG1655 LptD4213 (imp)	Outer-membrane permeable	0.004
MG1655 WT + 4mM EDTA	Outer-membrane permeable	0.002
MG1655 WT + 50% serum	Plasma protein binding	0.125
MG1655 WT + 1% surfactant	Lung inactivation	0.125
UPEC WT	WT	0.125
UPEC – LepB Low	Reduced LepB expression level	0.008
UPEC – LepB High	Increase LepB expression level	1

WT, wild type.

**Extended Data Table 2 | MIC values of G0775 measured against *E. coli* ATCC 25922 mutants that were generated spontaneously in response to plating on G0775 at 4 × MIC**

Background	Mutation	LepB residue, <i>E. coli</i> numbering	Fold MIC Increase
<i>E. coli</i> ATCC 25922	E83K	83	16
<i>E. coli</i> ATCC 25922	F85S	85	8
<i>E. coli</i> ATCC 25922	P88L	88	16
<i>E. coli</i> ATCC 25922	P88Q	88	4
<i>E. coli</i> ATCC 25922	P88R	88	16
<i>E. coli</i> ATCC 25922	P88T	88	4
<i>E. coli</i> ATCC 25922	V133F	133	16
<i>E. coli</i> ATCC 25922	L142R	142	8
<i>E. coli</i> ATCC 25922	D143Y	143	8
<i>E. coli</i> ATCC 25922	V149V-KRAV	149	128
<i>E. coli</i> ATCC 25922	A297V	297	4
<i>E. coli</i> ATCC 25922	AcrB (N282Y)	-	4

**Extended Data Table 3 | Cytotoxicity profile of G0775 against four different cultured mammalian cell lines**

Cell Line	IC <sub>50</sub> (μM)	Maximum % Inhibition at 50 μM
A549	>50	1.2
HEK-293T	>50	0.65
Jurkat	>50	-0.1
H23	>50	1.7

Cellular viability was measured after 3-day incubation of G0775 with each of the different cells by quantifying ATP levels as described in Supplementary Methods. The highest testing concentration was 50 μM.

## Reporting Summary

Nature Research wishes to improve the reproducibility of the work that we publish. This form provides structure for consistency and transparency in reporting. For further information on Nature Research policies, see [Authors & Referees](#) and the [Editorial Policy Checklist](#).

### Statistical parameters

When statistical analyses are reported, confirm that the following items are present in the relevant location (e.g. figure legend, table legend, main text, or Methods section).

n/a Confirmed

- The exact sample size ( $n$ ) for each experimental group/condition, given as a discrete number and unit of measurement
- An indication of whether measurements were taken from distinct samples or whether the same sample was measured repeatedly
- The statistical test(s) used AND whether they are one- or two-sided
  - Only common tests should be described solely by name; describe more complex techniques in the Methods section.*
- A description of all covariates tested
- A description of any assumptions or corrections, such as tests of normality and adjustment for multiple comparisons
- A full description of the statistics including central tendency (e.g. means) or other basic estimates (e.g. regression coefficient) AND variation (e.g. standard deviation) or associated estimates of uncertainty (e.g. confidence intervals)
- For null hypothesis testing, the test statistic (e.g.  $F$ ,  $t$ ,  $r$ ) with confidence intervals, effect sizes, degrees of freedom and  $P$  value noted
  - Give P values as exact values whenever suitable.*
- For Bayesian analysis, information on the choice of priors and Markov chain Monte Carlo settings
- For hierarchical and complex designs, identification of the appropriate level for tests and full reporting of outcomes
- Estimates of effect sizes (e.g. Cohen's  $d$ , Pearson's  $r$ ), indicating how they were calculated
- Clearly defined error bars
  - State explicitly what error bars represent (e.g. SD, SE, CI)*

*Our web collection on [statistics for biologists](#) may be useful.*

### Software and code

Policy information about [availability of computer code](#)

Data collection

Structural Biology: XDS was used for indexing and integration of diffraction data.

Data analysis

MIC: Excel  
Time-kill: Excel  
FOR: Excel  
Proteomics: Xcalibur Qual Browser  
Enzymology: GraphPad Prism and Dynafit  
Structural Biology: AIMLESS was used for scaling. Initial phases were obtained by molecular replacement using PHASER. Model building and refinement was achieved using Coot and the PHENIX suite of programs, respectively.  
Efficacy: GraphPad Prism

For manuscripts utilizing custom algorithms or software that are central to the research but not yet described in published literature, software must be made available to editors/reviewers upon request. We strongly encourage code deposition in a community repository (e.g. GitHub). See the Nature Research [guidelines for submitting code & software](#) for further information.

## Data

### Policy information about availability of data

All manuscripts must include a [data availability statement](#). This statement should provide the following information, where applicable:

- Accession codes, unique identifiers, or web links for publicly available datasets
- A list of figures that have associated raw data
- A description of any restrictions on data availability

-Whole genome sequencing data for CDC isolate 106 (genome and 2 associated plasmids) has been deposited into GenBank under accession codes CP022611, CP022612, and CP022613  
 - In vivo studies described in Figure 4 and Extended Data Figure 7 have associated raw data  
 - There are no restrictions on data availability

## Field-specific reporting

Please select the best fit for your research. If you are not sure, read the appropriate sections before making your selection.

Life sciences       Behavioural & social sciences       Ecological, evolutionary & environmental sciences

For a reference copy of the document with all sections, see [nature.com/authors/policies/ReportingSummary-flat.pdf](http://nature.com/authors/policies/ReportingSummary-flat.pdf)

## Life sciences study design

All studies must disclose on these points even when the disclosure is negative.

### Sample size

MIC, frequency of resistance & time-kill: The sample size was three independent replicates. The MIC values reported are the mode of the three replicates. The FOR and time kill values are the mean of the three replicates, and the error reported is the standard deviation. Sample sizes are consistent with similar experiments in the literature.  
 Proteomics: This study was performed twice, consistent with similar experiments in the published proteomics literature.  
 Enzymology: The Kinact/Ki determination was performed with quadruplicate data points and 3 separate experiments were performed to report the average values. Sample size is consistent with similar experiments in the published enzymology literature.  
 Structural Biology: A complete X-ray diffraction data set was collected on a single crystal.  
 Efficacy: The sample size was determined based on similar studies with neutropenic infection models (CFU) and mucin peritonitis models (survival) in the published antibiotic literature. The sample size is big enough to achieve statistical significance among groups for Mann-Whitney test for the CFU comparison and log-rank test for the survival comparison.

### Data exclusions

MIC, frequency of resistance & time-kill: No data was excluded from these studies.  
 Proteomics: No data was excluded from this study.  
 Enzymology: No data was excluded from this study.  
 Structural Biology: No data was excluded.  
 Efficacy: No data was excluded from this study.

### Replication

MIC: Against some of the standard strains such as E. coli ATCC 25922, MICs were measured multiple times over the course of many months as new batches of compound were synthesized. In all cases the MICs were within 2-fold of the reported values.  
 Time-kill: Other than the time kill data reported in the paper, one other time kill experiment was performed on E. coli 25922 with G0775, however only a single culture was used and no additional replicates were performed. This experiment was repeated using triplicate cultures. The data from the original experiment is not used in the paper, however, the trends between the data at each drug concentration in the two experiments are in agreement.  
 Frequency of resistance: Twelve additional FOR replicates were performed with E. coli at 4x MIC, and two additional replicates were formed at 8x and 16x MIC. Two additional FOR replicates were performed with K. pneumonia at 4x, 8x, and 16x MIC. All values were within the error reported. No additional replicates were performed with P. aeruginosa or A. baumannii.  
 Proteomics: Both attempts at this experiment were successful.  
 Enzymology: All 3 attempts at replication were successful. Kinact/Ki values from each of the 3 independent experiments were averaged and reported in the manuscript.  
 Structural Biology: Only a single crystal was generated in this study  
 Efficacy: All attempts at replication were successful.

### Randomization

MIC: There was no randomization  
 Time-kill: There was no randomization  
 FOR: There was no randomization  
 Proteomics: There was no randomization  
 Enzymology: There was no randomization  
 Structural Biology: A R-free set was used for cross-validation during model building and refinement  
 Efficacy: Mice were randomized based on their body weight before the infection.

## Blinding

MIC: There was no blinding  
 Time-kill: There was no blinding  
 FOR: There was no blinding  
 Proteomics: There was no blinding  
 Enzymology: There was no blinding  
 Structural Biology: There was no blinding  
 Efficacy: Blinding was achieved with data collection by personnel not familiar with the design or purpose of the study.

## Reporting for specific materials, systems and methods

### Materials & experimental systems

n/a	<input type="checkbox"/> Involved in the study <input checked="" type="checkbox"/> Unique biological materials <input type="checkbox"/> Antibodies <input type="checkbox"/> Eukaryotic cell lines <input checked="" type="checkbox"/> Palaeontology <input type="checkbox"/> Animals and other organisms <input checked="" type="checkbox"/> Human research participants
-----	--

### Methods

n/a	<input type="checkbox"/> Involved in the study <input checked="" type="checkbox"/> ChIP-seq <input checked="" type="checkbox"/> Flow cytometry <input checked="" type="checkbox"/> MRI-based neuroimaging
-----	--

## Unique biological materials

Policy information about [availability of materials](#)

Obtaining unique materials G0775, G3031, G8126 and G6850 are unique molecules proprietary to Genentech that are readily available on request.

## Antibodies

Antibodies used

Invitrogen, R960-25

Validation

Anti-V5 antibody was used in Extended Data Figure 7 (Invitrogen, R960-25). From Invitrogen's website: R960-25 recognizes amino acid sequence: -Gly-Lys-Pro-Ile-Pro-Asn-Pro-Leu-Leu-Gly-Leu-Asp-Ser-Thr-.

This antibody is functionally tested against 20ng of an E. coli expressed fusion protein containing a V5 epitope using a chemiluminescent substrate at a 1 minute exposure. This antibody has also been tested in Western blot against 25ng of recombinant Positope™ protein. The Positope™ control protein is a 53 kDa recombinant protein that contains seven epitope tags, including His (C-term), HisG, c-myc, and V5. Low background was observed using chemiluminescent or alkaline phosphatase reagents for detection. For Western blot, dilute in PBS or Tris-Buffered Saline (TBS) containing 0.05% Tween-20 and 5% nonfat, dry milk (PBSTM or TBSTM).

## Eukaryotic cell lines

Policy information about [cell lines](#)

Cell line source(s)

A549 (ATCC-CCL-185), Jurkat (ATCC-TIB-152), H23(ATCC-CRL5800) and HEK293T(ATCC-CRL-1573)

Authentication

Cell lines were purchased from ATCC and no authentication was performed

Mycoplasma contamination

These ATCC cell lines were not tested for mycoplasma contamination prior to assay.

Commonly misidentified lines  
(See [ICLAC](#) register)

No commonly misidentified lines were used in these studies.

## Animals and other organisms

Policy information about [studies involving animals; ARRIVE guidelines](#) recommended for reporting animal research

Laboratory animals

Neutropenic thigh infection model: CD1 female mice, 7 weeks old  
 Neutropenic lung infection model: Balb/c female mice, 7 weeks old  
 Mucin peritonitis model: CD1 female mice, 7 weeks old

Wild animals

The study did not involve wild animals.

